MINERAL EXPLORATION AND ALTERATION ZONE MAPPING IN EASTERN DESERT OF EGYPT USING ASTER DATA

Abduwasit Ghulam, PhD, Assistant Research Professor
Reda Amer, PhD Candidate
Department of Earth & Atmospheric Sciences and
Center for Environmental Sciences
Saint Louis University
St. Louis, MO 63103
ghulam@eas.slu.edu
ramer@slu.edu

Timothy M. Kusky, PhD, Distinguished Professor
Ministry of Education Three Gorges Geohazards Research Center, and
State Key Laboratory for Mineral Resources and Geological Processes
China University of Geosciences
Wuhan, Hubei 430074, China
tkusky@gmail.com

ABSTRACT

This paper proposes a method to find gold deposits in the Eastern Desert of Egypt. Different methods including various classification methods, principle component transform (PCT), band ratios, and a constrained energy minimization technique are evaluated for their performance for hydrothermal alteration zone mapping. First, these techniques are carried out to highlight known gold deposits over the Sukari Gold Mine. Then, the techniques are applied to different areas to search for sites that have similar spectral and other signatures in the processed images, with the idea that they may have conditions similar to those of the known gold deposits. Next, the newest methods in remote sensing of alteration zones and related minerals are discussed and compared with classic techniques, and the most effective techniques are identified. Finally, test sites using known gold deposits at Sukari and Abu Marawat are used to calibrate the techniques with the other gold concessions in the region. Results show that produced gold related alteration zone maps derived from newly developed methods in this research are in excellent agreement with known signatures of gold mines in the region and published geologic and minerals maps. The paper concludes that mineral information extraction based on n-dimensional spectral feature space analysis using the most sensitive wavelengths of altered minerals are the best method to map alteration zones associated with gold mineralization.

INTRODUCTION

Spectral discrimination of potential areas of gold mineralization (e.g. hydrothermal alterations and iron gossans) is a common application of remote sensing (e.g. Abdelsalam et al., 2000; Zhang et al., 2007). Many studies reported the extraction of spectral information related to gold-bearing alteration zones from different satellite sensors such as Landsat TM, Landsat Enhanced Thematic Mapper Plus (ETM+) and the Advanced Spaceborne Thermal Emission and Reflection Radiometer (ASTER). The use of different image processing techniques such as band rationing, principal component transform (PCT) and constrained energy minimization (CEM) have been reported by several authors (Loughlin, 1991; Ferrier et al., 2002; Crósta and Filho, 2003).

Nonlinear Image analysis techniques such as CEM and band ratios are based on the spectral characteristics of surface types. CEM highlights the target signature while suppressing background signals. Similarly, band ratioing can maximize the signal-to-noise ratio by suppressing the expression of topography (Sabins, 1997). Such expression demonstrates less variability over the spectral ranges in contrast to other land surface types. Most of the band ratio techniques are generally constructed using laboratory measured spectral profiles. However, laboratory measured spectra (e.g., USGS spectral library) does not exactly represent the actual field spectrum due to many uncontrolled factors that make the field conditions different from laboratory measurements. In addition, spectral unmixing usually requires detailed spectral profiles of each element in a mixed pixel, and this becomes the bottle-neck particularly for the use of middle-scale satellite data (Gabr et al., 2010). Therefore, developing techniques and methods purely based on the image spectra itself, will provide a simple yet efficient tool for features extraction.

The objective of this paper is to map hydrothermal alteration zones of gold mineralization in the North Eastern Desert (NED) of Egypt, and to discriminate them from altered zones with low-potential for gold mineralization. Toward this end, we attempt to evaluate existing techniques for their performance over a known gold mine locality in the South Eastern Desert (SED) of Egypt – the Sukari gold mine (24.95526 N, 34.720242 E), because of the presence of old gold workings in that area. The selected techniques which successfully identified the known Sukari Gold Mine are then used to detect alteration zones over the other study area – Abu Marawat in NED of Egypt. Remote sensing derived alteration signatures are then further investigated against its potential for gold prospectus by integrating tectonic setting and geological mechanisms relevant for gold mineralization.

STUDY AREA

Two test sites are used in this study. The Sukari gold mine (Helmy, et al., 2004) is located in a mountainous area of the SE Desert of Egypt and was used to test and evaluate different methods planned to be used in the Abu Marawat area, with the idea that the broadly similar geology at Abu Marawat may host similar deposits to Sukari. The selected techniques which successfully identified the known Sukari Gold prospect are then used to detect alteration zones over the other study area—Abu Marawat (Figure 1).

Both study areas are located in the Eastern Desert (ED) of Egypt which is a part of the Arabian Nubian Shield (ANS). The ANS was formed by accretion of island arcs, accretionary prisms, back arc basins, and continental micro plates during the Pan-African orogeny about 600 Ma ago (Stern, 1994; Kusky et al., 2003). The Eastern Desert of Egypt is almost exclusively built up of ophiolitic mélange and associated rocks, accreted arcs, together with subordinate molasse-type sediments and late-tectonic volcanics and granitoid intrusives (El Ramly et al., 1993). The Sukari and Abu Marwat areas have two among many of old gold mines in the eastern desert of Egypt that has been exploited since Pharaonic and Romanian times. The revolution of exploration and exploitation techniques and also the high prices of gold in the last few decades lead the Egyptian Mineral Resources Authority (EMRA) to develop the old gold mines and explore new sites of gold mineralization.

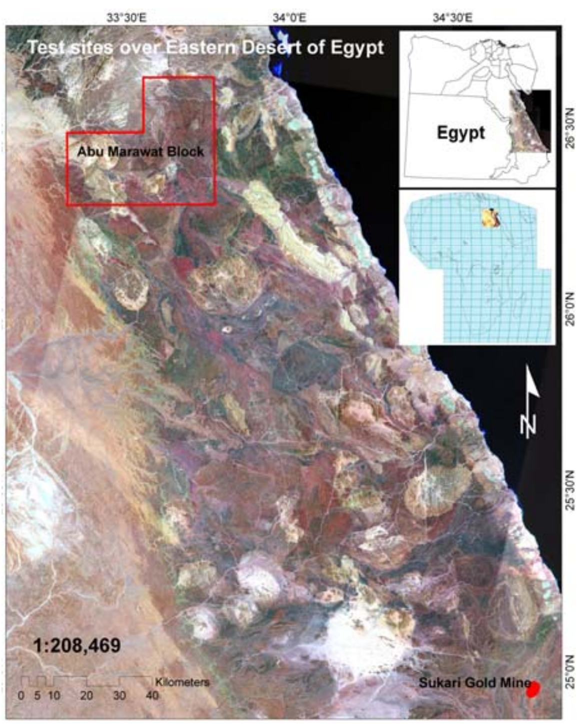

Figure 1. Location map of Sukari Gold Mine and Abu Marawat concession block on a Landsat ETM+ (7, 4, 2) false color mosaic image of eastern desert of Egypt.

METHODS

Data and Pre-processing

The geologic Map of Jabal Hamatah Quadrangle, 1997 (scale 1:250000) from the Geological Survey of Egypt, Ministry of Industry and Mineral Resources is used to validate results from remote sensing data. The Advanced Spaceborne Thermal Emission and Reflection Radiometer (ASTER) data collected over both test sites- Sukari and Abu Marawat- represent the final surface reflectance image scaled between 0-1000. Radiometric and atmospheric correction was done by the NASA data Distribution Center.

Brief Description of Candidate Methods

Different techniques including various classification methods (e.g., supervised and unsupervised), decorrelation analysis, non-linear image enhancement techniques including band ratios, and PCT, have been performed at the Sukari mining area as a pilot study to indentify and validate the most effective method. The most successful technique indentified was then applied to other study locations where further high-potential targets are expected. A brief introduction to some of these methods is given in the following sections.

Band Ratios. Band Ratios were used to enhance the spectral differences between bands and to reduce the topographic effects. Dividing one spectral band by the other produces an image that provides relative band intensities. A thorough description of the selection of sensitive bands for minerals can found in relevant publications (e.g., Sabins, 1999). We selected Sabin's Ratio (5/7, 3/1, 3/5 in RGB) (Sabins, 1997) and Abram's ratio (5/7. 4/5, 3/1 in RGB) (Abrams, 1983) for candidate band ratios. These band numbers are for ETM+ data. Similar wavelength regions for ASTER data can be chosen according to the bandwidths to generate ratio maps from ASTER data.

Principle component transformation of mineral indices. The PCT technique (Pearson, 1901) is a mathematical procedure widely used in the image processing industry today that transforms a number of correlated spectral bands into a smaller number of uncorrelated spectral bands called principal components. This is done by finding a new set of orthogonal axes that have their origin at the data mean and that are rotated so the data variance is maximized. The first component is in the direction of the greatest variance in the dataset, the second component is in the direction of the second greatest variance in the data set, and so forth. Therefore, PCT helps to enhance and separate certain types of spectral signatures from the background. However, PCT of individual spectral bands is not capable of eliminating topographic and atmospheric effects due to the fact that it is simply a rotation of spectral feature space to the directions of maximum variance. Therefore, we used the combination of band ratio images (Ninomiya, 2003) and the PCT transforms following Zhang et al. (2007).

Constrained Energy Minimization (CEM). The constrained Energy Minimization (CEM) technique (Harsanyi, 1993) performs a matched filtering (MF) of hyperspectral/multispectral images, then linearly constrains a desired target signature while minimizing other unknown signatures where the only required knowledge is the training target spectra to be provided as user end members. Using partial unmixing based on the estimate of sample correlation matrix highlights target abundances. Therefore, the contrast between target spectra and the background are enhanced by maximizing the response of the known end members while suppressing the response of the composite unknown background. The ability of this technique to deal with mixed background spectra and to accommodate that nonlinear mixing among them is a major advantage for the CEM over PCT transformed mineral indices discussed in the previous section.

Spectral unmixing in n-dimensional spectral feature space. To separate minerals between each cell, we implemented a partial spectral unmixing method based on the 'Spectral Hourglass' scheme (Kruse et al., 2003) available in ENVI 4.7 (ENVI® image processing and analysis software, from ITT Visual Information Solutions). This method starts with reducing abundant information and data dimensionality using the Minimum Noise Fraction (MNF) transform then subsequently applies, Pixel Purity Index-Mapping (PPI) for the determination of the purest pixels in the image and the extraction of end-members utilizing the n-Dimensional-Visualizer tool (n-D-Vis). The extracted end-members are then compared to known spectra from USGS spectral libraries to further indentify and prepare for the Spectral Angle Mapper (SAM) classification (Kruse et al., 1993). This method is one of the widely accepted and popular image processing techniques for hyperspectral image processing. However, it may not be optimal for multispectral data. In our case with ASTER data, the majority of the pixels were somehow removed by the scheme. Therefore, we used byproducts generated during the processing scheme, namely, the spectrally matched score images.

The ASTER spectral library (Version 1.2, http://speclib.jpl.nasa.gov) has been used to identify the four alteration minerals (alunite, kaolinite, montmorillonite and muscovite) from the VNIR/SWIR surface reflectance data. The reference spectra of these four minerals (Figure 2a) were extracted from the USGS spectral library. The spectral library is ideal tool for hyperspectral analysis with hundreds of bands. Yet, we don't have many choices except the VNIR and SWIR bands of ASTER data. Since the sensor specific reflectances are often available at broadband wavelengths and subject to varying sensitivities over the wavelengths, the spectra from USGS spectral library should be convolved with the spectral response function of ASTER wavebands (Figure 2b). It can be seen from Figures 2a and b that the altered minerals have a strong absorption in SWIR region, located at band 6 and 8 of ASTER data. Minerals also indicated a strong reflection over VNIR band and one of the SWIR bands (band 4). However, the alunite spectrum overlaps with other minerals in VNIR region. Therefore, the most sensitive bands of the minerals may be bands 4, 6, and 8. The spectra of kaolinite with alunite and muscovite with montmorillonite are very similar. Further analysis using a continuum removal technique revealed that these minerals may be further classified using band 6 (good to separate alunite and kaolinite) and band 8 (good to separate the other two minerals) as shown in Figure 2c.

a

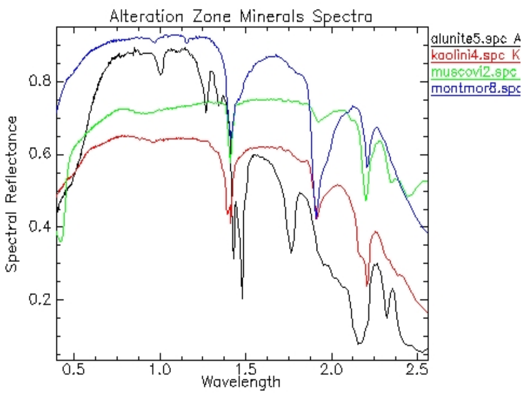

b

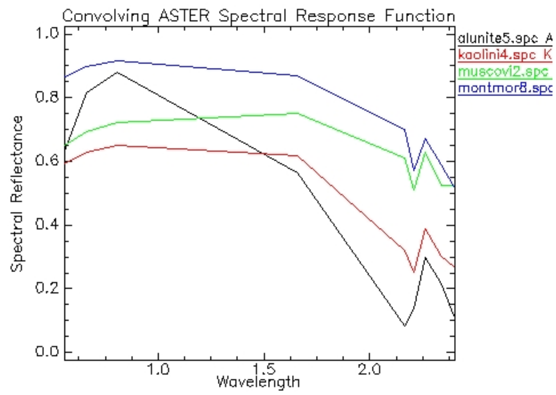

c

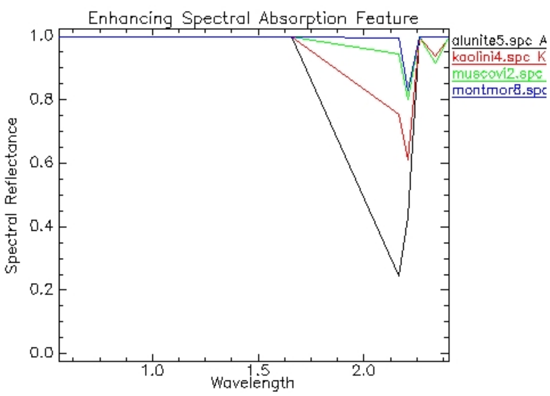

Figure 2. Convolution of USGS spectral library profiles with ASTER spectral response function using ENVI: 2a refers the USGS spectra for the alteration minerals; 2b shows the spectral curves after convolved with ASTER sensor spectral response function; 2c represents the spectral curve after continuum removal.

As described in previous sections, matched filtering, minimum noise transform, and absorption feature enhancement techniques were implemented. Next, n-dimensional spectral feature spaces have been implemented to map these minerals (Figure 4) using the Mixture Tuned Matched Filtering (MTMF) images, then PCT is applied to MTMF images to further highlight the desired signal while reducing information redundancy. Figure 3a shows a 2-dimensional scatter plot of montmorillonite and kaolinite, and deviation of alteration zone minerals (Figure 3b) from the background pixels (Figure 3c). There are critical values where vectors of alteration minerals separate from the background signal in the developed spectral feature space. These critical boundary values are determined using n-dimensional spectral feature spaces developed from each of the alteration minerals, respectively.

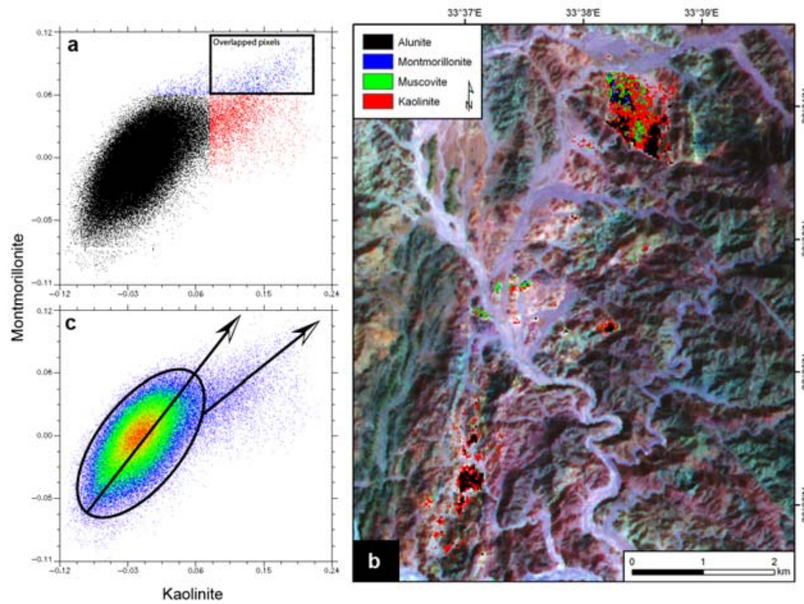

Figure 3. Indentifying alteration minerals using n-dimensional spectral feature space.

RESULTS AND DISCUSSIONS

Sukari Case Study

The Sukari area is occupied by Pan-African rocks represented by dismembered ophiolites,, metavolcano-sedimentary rocks, and granodiorite. The dismembered ophiolitic succession is represented by serpentinite, metagabbro, and sheeted dykes (El Sharkawy and El Bayoumi 1979). The metavolcanics and volcaniclastics are composed of andesites, dacites, tuffs, and pyroclastics (Akaad et al 1995). The granodiorite intrudes the ophiolitic and metavolcanic rocks and is composed of quartz, plagioclase, K-feldspar and biotite (Helmy et al 2004). The Sukari area has been subjected to sinistral strike-slip and normal faulting which helped hydrothermal fluid flow and hosts gold bearing quartz veins. The granodiorite hosts the Sukari gold mine and is dissected by numerous quartz veins some of which have gold mineralization and trend (N-S, NNE-SSW) and some are barren, typically striking NW-SE (Helmy et al 2004). Quartz veins associated with alteration zones vary in thickness from few centimeters to tens of meters according to the thickness of quartz vein (Helmy et al 2004).

We tested all of the abovementioned methods on the known Sukari gold prospect. Figure 4: a is Abrams's ratio; b) is Sabin's ratio, and c) is PCT of minerals indices, d) is the PCT from reflectance data (PC1, 2, 3 in RGB), e) is PCT based on MTMF (PC1, 2, 4 in RGB) and, f) shows the detected alteration zones in red and highlighted structural lineaments as the background image using spectral unmixing in n-dimensional spectral feature space. It becomes clear that there is still a significant shadow effect in the results derived from classic image processing techniques including band ratios, supervised and unsupervised classifications with various classifiers and principle component transform (PCT) of reflectance data. The sunlit and the shaded sides of the mountains (e.g., over the Sukari Gold mine which resides mainly in granite rocks) show very different spectral signatures even with band ratios in which topographic effects are expected to be minimized. However, these methods well identify rock units in the study area. As shown in Figure 4c, principle transform of mineral indices showed some promise in detecting the shear zone where main gold mining activities have been conducting over Sukari Gold Mine. It is difficult to identify these features and signatures, though, from the minerals abundance images based on MTMF or PCT form of MTMF (Figure 4e). Spectral unmixing in n-dimensional spectral feature space provides a flexible approach to indentify alteration zone minerals. As shown in Figure 4f, indentified locations in red confirm the Sukari Gold Mine and gold localities based on the geologic maps from the Geological Survey of Egypt. Some other indentified alteration zones that do not fall upon gold-bearing rock units according to the geologic map suggests that further analysis integrating petrographical and fluid inclusion data, regional tectonic setting and geologic mechanisms relevant to shear zones, fractures, and dikes need to be performed on each alteration zone locality from remote sensing image processing.

It is evident from Figure 4f that "rule" images generated from MTMF process and its certain color composites are useful to enhance geologic structural lineaments, and shear zones that are critical next-step indicators to indentify gold bearing alteration zones. The results are in conformity with tectonic settings and the geologic structure of the area as described in the previous paragraph.

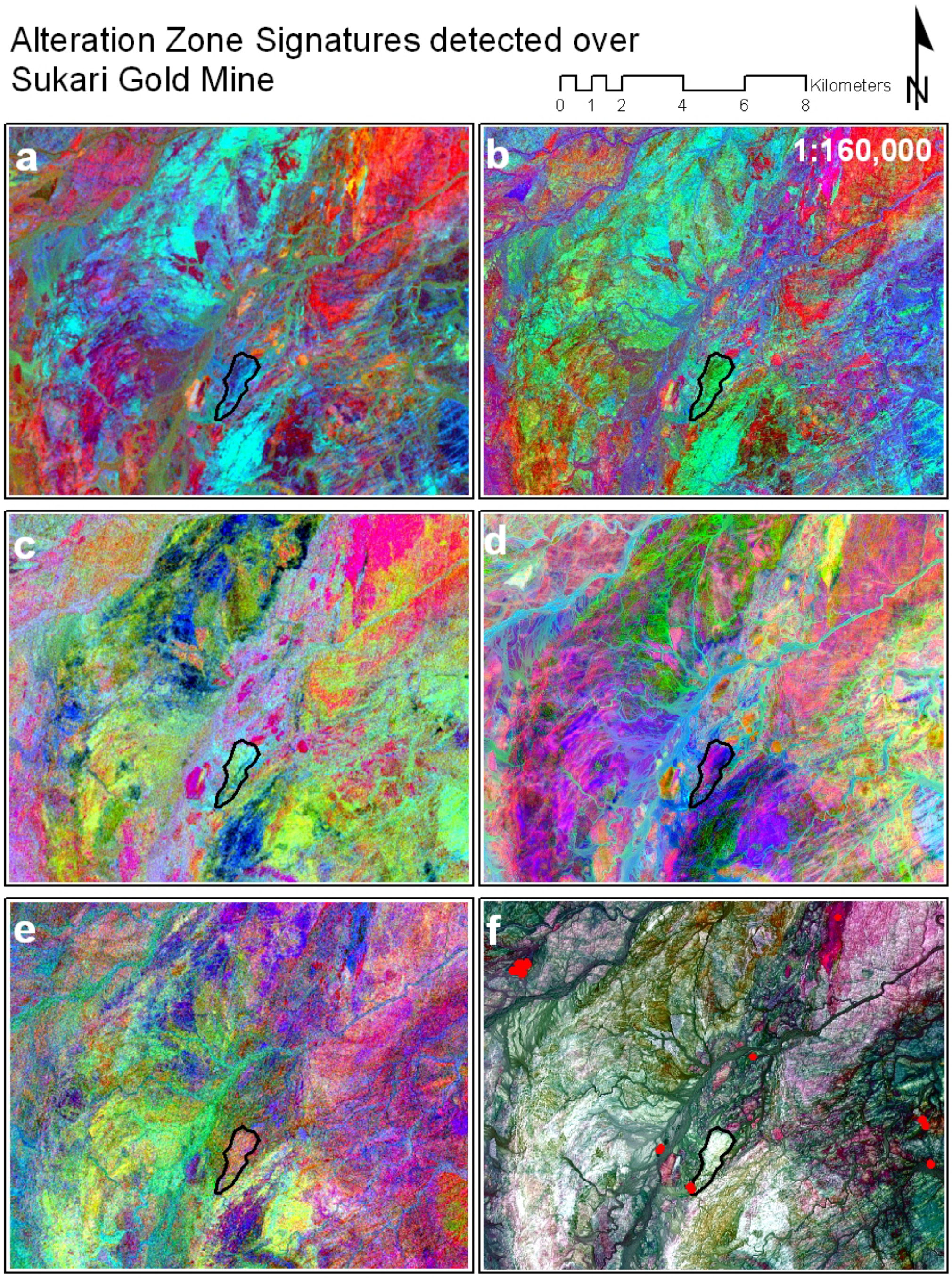

Figure 4. Detected alteration zone signatures from various methods over the Sukari Gold Mine. a) Abram's ratio, b) Sabin's ratio, c) PCT transform of minerals indices, d) principle component transform of spectral reflectance bands, e) principle component transform of minerals abundances derived from spectral unmixing in n-dimensional spectral feature space, and f) identified alteration zone minerals from SAM classification (in red) and enhanced structural and linear geologic features.

Abu Marawat Case Study

Abu Marwat area is also covered by Pan-African igneous and metamorphic rocks represented by dismembered ophiolites, metasediments, metavolcanics, older granite (granodiorite), and younger granite (alkali granite). The area is dissected by numerous faults and shear zones striking in different directions, some of which are filled with quartz veins and accompanied by gold mineralization. The area under investigation hosts four significant gold occurrences in the ED of Egypt including Abu Marawat, Semna, Erediya and Hamama (Figure 5). The gold mineralization occurs in gold bearing quartz veins associated with alteration zones in granitic rocks in three locations Semna, Eradiya and Hamama. Gold mineralization associated with oxide facies Banded Iron Formation (BIF) overlying the metavolcaniclastics was found at Abu Marawat gold prospect (Botros, 1993).

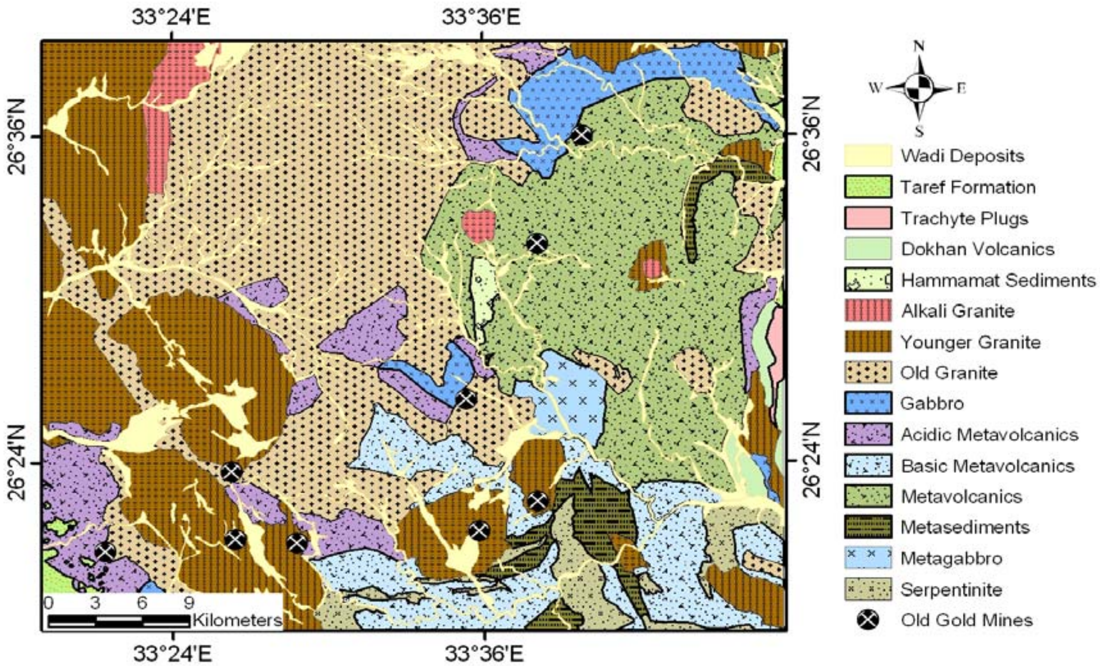

Figure 5. Geologic map of Abu Marwat area.

Remote sensing analysis was done to see if the methods were able to pick up the spectral signature and identify the alteration zones of gold bearing BIF overlying the metavolcaniclastics in Abu Marawat area. As shown in Figure 6, alteration zone signatures in yellow from the two methods, i.e., PCT transform of mineral indices, spectral unmixing in n-dimensional spectral space, are quite similar in terms of mineral abundance and macro spatial patterns of alteration zone minerals indentified except for subtle deviations in microscale texture. The reason for this may be that both methods perform PCT transformations on the basis of minerals enhanced by mineral indices in the first case, and enhanced minerals signatures from MTMF. This case study shows that these two methods are good tools for analyzing ASTER reflectance data producing sharper and more focused results. Comparing spectral unmixing using n-dimensional feature space and PCT of the mineral indices, alteration zones were clearly identified without any noise or spectral disturbances from other minerals particularly with the former method. In addition, the former method enabled us to emphasize geologic features by simply using a color composite of its by products – "rule" images generated during the 'Spectral Hourglass' scheme. CEM did not perform well in the conditions where the background signature was not easily detected, and therefore, was unable to separate signatures that were not spatially dominant in the image.

A final color composite image as a result of the n-dimensional spectral space method was generated using matched filtering score images – byproducts (not the final products) of the 'Spectral Hourglass' scheme. The final product, however, generated with the processing chain was nothing than an image with countable pixels that do not fall on any alteration zone prospects. Most of the pixels were somehow removed during the process in our case. Further studies are needed to find out the reason for this result.

The best results obtained by various combinations of band ratios showed some promise to detect alteration zones, but failed to discriminate altered minerals from wadi deposits and sedimentary rocks. For example in Figure 7a, the three "Kidney" shaped sedimentary rock units in the central- right and upper-right sides of the image produced quite similar signatures (yellow color) with alteration zones (circles #1 and 3). This kind of "spectral confusion" was also found in the central part of the ratio image as shown circles #2, 4-5 while it is clearly discriminated by our method (Fig. 7b).

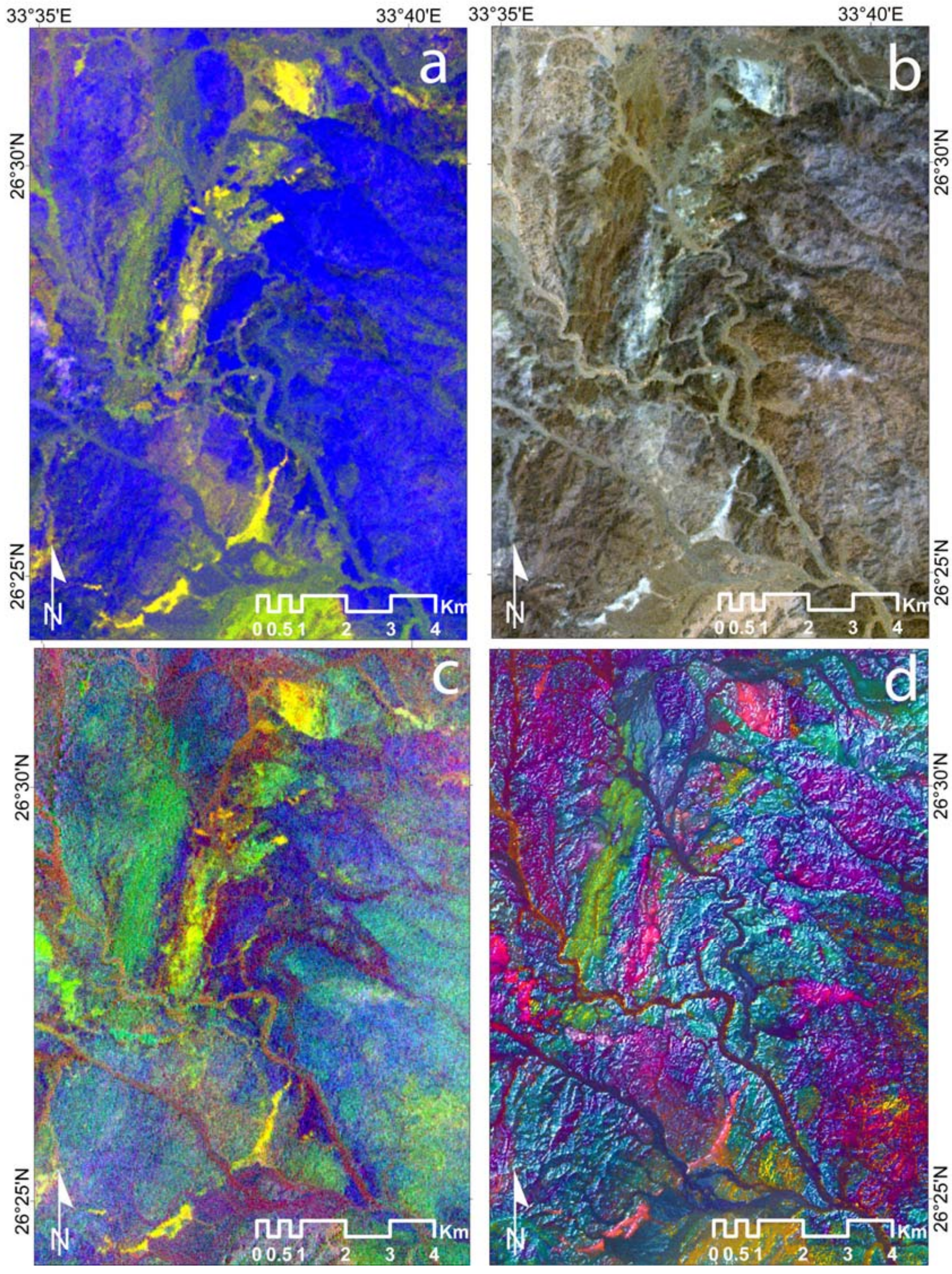

Figure 6. Alteration zone prospects from different methods: 6a is the PCT transform of the mineral indices in which the yellow represents alteration zones; 6b is from the CEM technique, 6c is PCT transform of minerals separated using n-dimensional spectral feature space (alteration zones are in yellow), and 6d is color composited "rule" images of 'Spectral Hourglass' scheme corresponding 4, 6, 8 bands in RGB.

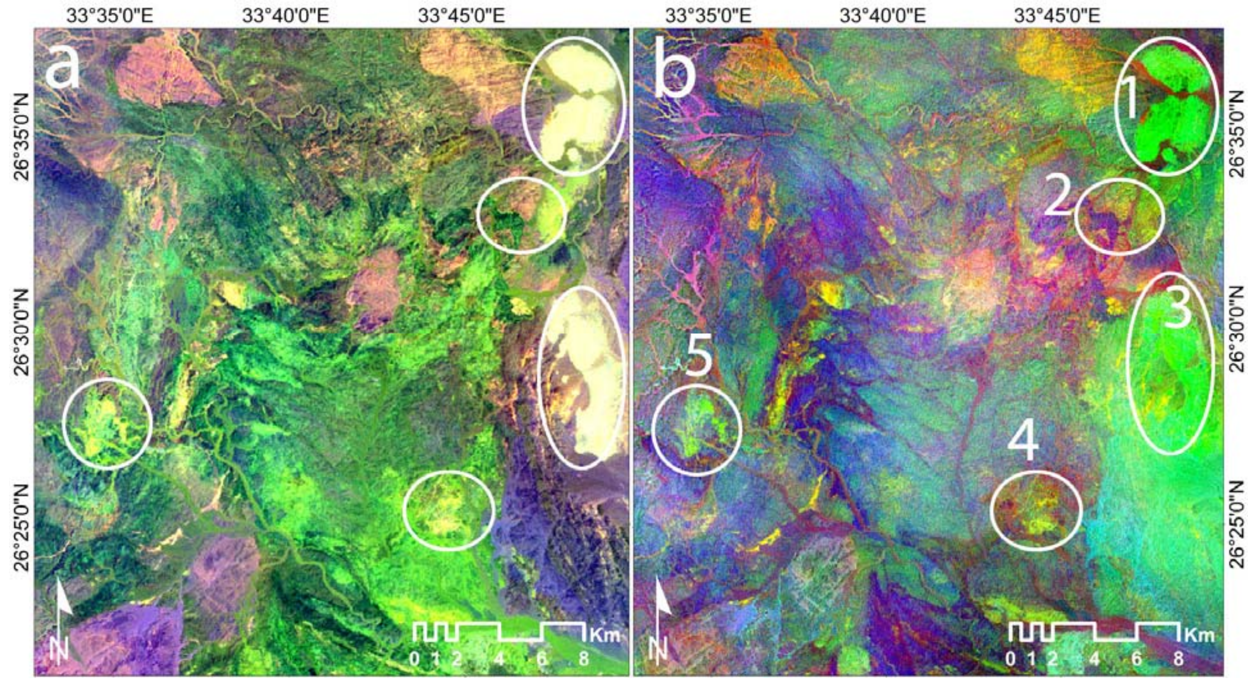

Figure 7. Spectral discrepancies between the results of spectral unmixing in n-dimensional spectral space and band ratios. Figure 7a is the best result achieved by various combinations of band ratio products, 7b is the image obtained by spectral unmixing in n-dimensional spectral feature space. The three "kidney" shaped rocks in the central- right and upper-right sides of the images are clearly separated in latter while they show quite similar signatures (color) with alteration zones in the ratio image.

CONCLUSION

Overall, two of the outlined methods in the paper including PCT of minerals indices, PCT of MTMF components and spectral unmixing in n-dimensional spectral feature space show promise to extract alteration zones. Results are very similar between the different methods and indices implemented, suggesting the highlighted areas are altered and mineralized. However, spectral unmixing in n-dimensional spectral space more effectively shows the mineral abundance. Alteration zones are clearly extracted without any noise and disturbances. In addition, the method enables one to extract individual minerals using critical threshold values developed in the methods section. The resulting alteration minerals abundance image has been found to be sharper and easier to interpret than the image produced by the PCT transform of mineral indices.

The CEM technique, however, did not perform well in conditions where the background signature is not easily detected, therefore, fails to indentify rare minerals (e.g. secondary iron-rich parts of the alteration) that are not spatially dominant in the image. In other words, it is problematic to enhance the target spectra while minimizing background "energy" using CEM when there is no apparent difference between the target and background spectral signatures.

ACKNOWLDGEMENTS

This work was supported by the Open foundation of the Ministry of Education Key Laboratory of Oasis Ecology of Xinjiang (No. XJDX0201-2008-01). Additional funds were provided by the National Natural Science Foundation of China (Grant 40821061) and the Ministry of Education of China (B07039).

REFERENCES

Abdelsalam, M.G., Stern, R.J. and Berhane, W.G., 2000. Mapping gossans in arid regions with Landsat TM and SIR-C images: the Beddaho Alteration Zone in northern Eritrea. *Journal of African Earth Sciences*, 30: 903-916.

Abrams, M.J., Brown, D., Lepley, L., Sadowski, R., 1983. Remote sensing of porphyry copper deposits in Southern Arizona. *Economic Geology,* 78 (4): 591–604.

Akaad, M.K., Noweir, A.M., Abu El Ela, A.M., 1995. The volcano-sedimentary association and ophiolites of Wadi Mubarak, eastern Desert, Egypt. Proc. Int. Conf. 30 years cooper. *Geol. Surv. Egypt Spec. Publ.*, 69: 231-248.

Botros, N.S., 1993. The possible occurrence of placer gold in areas lacking quartz veins in Egypt. *J. Geochem. Explor.*, 49:287-290.

Crósta, A.P. and Filho, C.R.d.S., 2003. Searching for gold with ASTER. *Earth Observation Magazine*, 12: 38-41.

El Ramly, M.F., Greiling, R.O., Rashwan, A.A. and Rasmy, A.H., 1993. Geologic map of Wadi Hafifit area. Scale 1:100.000, *Egyptian Geological Survey* (1993), p. 68.

El Sharkawy, M.A., and El Bayoumi, R.M., 1979. The ophiolites of Wadi Ghadir area, Eastern Desert, Egypt, *Annals of the Geological Survey of Egypt*, 9:125–135.

Ferrier, G., White, K., Griffiths, G. and Bryant, R., 2002. The mapping of hydrothermal alteration zones on the island of Lesvos, Greece using an integrated remote sensing dataset. *International Journal of Remote Sensing*, 23: 341-356.

Gabr, S., Ghulam, A., and Kusky, T., in review. Detecting areas of high-potential gold mineralization using ASTER data. *Ore Geology Reviews*, (revised)

Harsanyi, J.C., 1993. Detection and Classification of Subpixel Spectral Signatures in Hyperspectral Image Sequences. *Ph.D. Dissertation, University of Maryland, Baltimore County*: 116 pp.

Helmy, H.M., Kaindl, R., and Fritz, Harald, 2004. The Sukari Gold Mine, Eastern Desrt-Egypt: structural setting, mineralogy and fluid inclusion study. *Mineralium Deposita*, 39: 495-511.

Kruse, F.A., Boardman, J.W. & Huntington, J.F., 2003. Comparison of Airborne Hyperspectral Data and EO-1 Hyperion for Mineral Mapping. *IEEE Transactions on Geoscience and Remote Sensing*, 41(6): 1388-1400.

Kruse, F. A., A. B. Lefkoff, J. B. Boardman, K. B. Heidebrecht, A. T. Shapiro, P. J. Barloon, and A. F. H. Goetz, 1993. The Spectral Image Processing System (SIPS) - Interactive Visualization and Analysis of Imaging spectrometer Data. *Remote Sensing of Environment*, 44: 145-163.

Kusky, T.M., Adelsalam, M., Stern, J.S. and Tucker, R.D., 2003. Evolution of the East African and related orogens, and the assembly of Gondwana. *Precambrian Research,* 123: 81-85.

Loughlin, W.P., 1991. Principal component analysis for alteration mapping. *Photogrammetric Engineering and Remote Sensing*, 57: 1163-1169.

Ninomiya, Y., 2003. A stabilized vegetation index and several mineralogic indices defined for ASTER VNIR and SWIR data. *Proceedings of IEEE 2003 International Geoscience and Remote Sensing Symposium. IGARSS'03*, 3, 1552-1554.

Sabins, F.F., 1997. Remote Sensing principles and interpretation. W. H. Freeman Company, New York, 366-371 pp.

Stern, R.J., 1994. Arc assembly and continental collision in the Neoproterozoic East African Orogen: implications for the consolidation of Gondwanaland. *Annual Review of Earth and Planetary Sciences,* 22: 319-351.

Takla M.A., El Dogdoug A.A., Rasmy A.H., Gad M.A., El Tabbal H., 1990. Origin of Um Eliega gold mineralization, South Eastern Desert, Egypt. *Egyptian J Mineral*, 2:3-20

Zhang, X., Pazner, M. and Duke, N., 2007. Lithologic and mineral information extraction for gold exploration using ASTER data in the south Chocolate Mountains (California). *Photogrammetry & Remote Sensing*, 62: 271-282.